Geomechanics and Engineering, *Vol. 19, No. 6 (2019) 513-522*
DOI: https://doi.org/10.12989/gae.2019.19.6.513

Elasto-plastic solution for cavity expansion problem in anisotropic and drained soil mass

Chao Li[a], Jin-feng Zou[b] and Liang Li*

School of Civil Engineering, Central South University, Hunan 410075, China

(Received October 31, 2018, Revised November 19, 2019, Accepted December 2, 2019)

Abstract. This study presents an elasto-plastic (EP) solution for drained cavity expansion on the basis of unified strength failure criterion and considers the influence of initial stress state. Because of the influence of initial consolidation of soil mass, the initial stress may be anisotropic in the natural soil mass. In addition, the undrained hypothesis is usually used in the calculation of cavity expansion problem, but most of the cases are in the drained situation in practical engineering. Eventually, the published solution and the presented solution are compared to verify the suitability of the study.

Keywords: elasto-plastic solution; drained cavity expansion; unified strength failure criterion; initial stress state

1. Introduction

Cavity expansion theory (CET) has been widely used in civil engineering, for problem such as pile foundations, grouting, underground engineering and in-situ test, and so on. Different failure criterion and model were applied to investigate and analyze the cavity expansion mechanisms, and considered the unloading cases. Some CET were as follows in geotechnical engineering field: Theoretical research (Hill 1950, Vesic 1972, Carter *et al.* 1979, 1986, Yu 2000, Park *et al.* 2008, Silvestri and Abou-Samra 2012, Wang *et al.* 2012a, b, Chen and Abousleiman 2013, Yang and Pan 2015, Li *et al.* 2016, Mo and Yu 2016, Xiao *et al.* 2016, Mo and Yu 2017a, b, Zou *et al.* 2017, Zhou *et al.* 2018, Zou and Wei 2018, Li *et al.* 2019a, b); Engineering applications (Randolph 2003, Zhang *et al.* 2013, Zhang *et al.* 2015a, b, Zhou *et al.* 2017, Peng *et al.* 2018, Zou *et al.* 2018, Chen *et al.* 2019a, b, Zhao *et al.* 2019, Zou *et al.* 2019, Zou and Zhang 2019); Numerical simulations and experiments (Teh and Houlsby 1991, Salgado and Prezzi 2007, Tolooiyan and Gavin 2011, Seo *et al.* 2012, Marchi *et al.* 2014, Mo *et al.* 2016); and others.

However, most of the above-mentioned published papers for CET were mostly based on the isotropic and undrained failure criterion, which is not consistent with field situation in practice. Because of the initial consolidation of soil mass, and the initial stress may be anisotropic in natural soil mass (Anderson 1980, Li *et al.* 2016). In addition, in order to simplify calculation, the assumption of undrained case was usually used in the most of the theoretical calculation, however, most of the field situation were in the drained situation in practical engineering. Only a few published results presented a theoretical solution considering the influence of initial stress anisotropy and drained case in saturated soil mass. Russell and Khalili (2002) proposed a similarity solution for cavity expansion problem based on the Mohr-Coulomb failure criterion to investigate and analyze the sand behavior. Chen and Abousleiman (2013) proposed an exact elasto-plastic theoretical solution for cylindrical cavity expansion problem based on the modified Cam-clay (MCC) model consider drainage case. The K_0-based modified Cam-clay (K_0-MCC) model (Li *et al.* 2016) was applied for the analysis of natural soil mass, an approximate closed-form solution was proposed for practical purposes, and the influence of initial stress anisotropy was reflected by employing the coefficient of K_0 in the paper.

Meanwhile, with the development of failure criterion and model, CET in a more advanced soil mass model (UST model) is necessary (Yu, 2004). The unified strength failure criterion is introduced into analyze the cavity expansion mechanisms, it has been widely applied in engineering practices because of it has a unified model and a simple unified mathematical expression.

In summary, most of the above-mentioned published papers for CET were mostly based on the isotropic and undrained failure criterion and model, which is not consistent with field situation in practice. The main objective of this paper is to develop a theoretical solution, on the basis of unified strength failure criterion and considering the influence of initial stress anisotropy and drained case. Eventually, the published case and the parametric studies are presented to verify the suitability of the theoretical solution, and the influence of initial stress anisotropy is reflected by employing the coefficient b in the study.

*Corresponding author, Professor
E-mail: liliang_csu@126.com
[a]Ph.D. Student
E-mail: lichao@csu.edu.cn
[b]Professor
E-mail: zoujinfeng_csu@163.com

ISSN: 2005-307X (Print), 2092-6219 (Online)

2. Theory and methodology

2.1 Problem definition and assumptions

2.1.1 Problem definition

In order to simplify analysis, the cavity can be divided to two zone: the elastic zone and the plastic zone. σ_{h0} is the initial in-situ horizontal stress, a_0 is the initial internal radius. With the increase of the internal pressure p, the first yield appeared in the wall of the cavity, a is the corresponding expanding radius. r_p is the position of the EP boundary, and the final radius of the cavity is a_u. The radial displacement of the EP boundary is u_{rp}. The schematic diagram of cavity expansion is shown in Fig. 1.

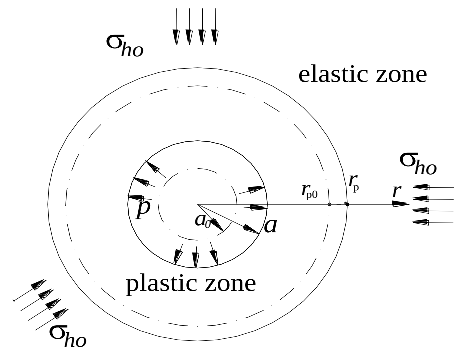

Fig. 1 Mechanical model for cavity expansion problem

2.1.2 Assumptions

Some assumptions can be written:

(1) Yu (2004) proposed a unified strength failure criterion, it has been widely applied in engineering practices because of it has a unified failure criterion and a simple unified mathematical expression. The unified strength failure criterion can be written,

$$f = \sigma_r - R\sigma_\theta - \sigma_0 = 0 \tag{1}$$

$$R = \frac{2(1+b)(1+\sin\varphi) + mb(\sin\varphi - 1)}{[2(1+b) - mb](1-\sin\varphi)} \tag{2}$$

$$\sigma_0 = \frac{4(1+b)c\cos\varphi}{[2(1+b) - mb](1-\sin\varphi)} \tag{3}$$

where c and φ are cohesion and internal friction angle, respectively, b is coefficient reflecting the influence of the intermediate principal stress on the yielding of the material ($0 \le b \le 1$), m is coefficient of the intermediate principal stress. Under the case of plane strain, when the soil mass is in the plastic region, $m \to 1$. It is assumed in the following calculation in the plastic region that $m \approx 1$.

(2) The small-strain can be written, $\varepsilon_r = du/dr$, $\varepsilon_\theta = -u/r$. The large-strain can be written, $d\varepsilon_r = -\partial (dr)/\partial r$, $d\varepsilon_\theta = -(dr/r)$.

2.2 Elastic-plastic solution of cavity expansion

In both elastic and plastic region, the equilibrium equation can be written,

$$\frac{d\sigma_r}{dr} + \varsigma \frac{\sigma_r - \sigma_\theta}{r} = 0 \tag{4}$$

where σ_r and σ_θ are the radial stress and the tangential stress, respectively.

2.3 Elastic region

The stress and displacement of soil mass in elastic zone can be written,

$$\sigma_r = \sigma_{h0} + (\sigma_{rp} - \sigma_{h0})\left(\frac{r_p}{r}\right)^{\varsigma+1} \tag{5}$$

$$\sigma_\theta = \sigma_{h0} - \frac{(\sigma_{rp} - \sigma_{h0})}{\varsigma}\left(\frac{r_p}{r}\right)^{\varsigma+1} \tag{6}$$

$$u = \frac{(1+\nu)(\sigma_{rp} - \sigma_{h0})r_p}{\varsigma E}\left(\frac{r_p}{r}\right)^{\varsigma} = \frac{(\sigma_{rp} - \sigma_{h0})r_p}{2\varsigma G}\left(\frac{r_p}{r}\right)^{\varsigma} \tag{7}$$

where ζ indicating form of cavity (=1, cylindrical; =2, spherical).

In EP boundary, the displacement of soil mass around the cavity can be written,

$$u_{rp} = \frac{(1+\nu)(\sigma_{rp} - \sigma_{h0})r_p}{kE} = \frac{(\sigma_{rp} - \sigma_{h0})r_p}{2kG} \tag{8}$$

The boundary conditions can be written,

$$\left.\begin{array}{l} \sigma_r(r = r_p) = \sigma_{rp} \\ \lim\limits_{r\to\infty} \sigma_r = \sigma_{h0} \end{array}\right\} \tag{9}$$

2.4 Elasto-plastic boundary analysis

In order to determine the plastic zone, namely, the radius of the plastic zone (r_p). Following the similarity solutions of Yu and Carter (2002), the radius of the plastic zone (r_p) in drained case is calculated as follows. According to Eq. (1), this yield condition can be also expressed,

$$\begin{aligned} \sigma_r &= R\sigma_\theta + \sigma_0 \\ &= \frac{2(1+b)(1+\sin\varphi) + mb(\sin\varphi - 1)}{[2(1+b) - mb](1-\sin\varphi)}\sigma_\theta \\ &+ \frac{4(1+b)c\cos\varphi}{[2(1+b) - mb](1-\sin\varphi)} \end{aligned} \tag{10}$$

Following Yu and Carter (2002), which similarity solutions assumed that the cavity pressure is constant, and the continuous deformation is geometrically self-similar.

The non-associated flow rule can be written,

$$\frac{d\varepsilon_{rp}^p}{d\varepsilon_{\theta p}^p} = \frac{d\varepsilon_{rp} - d\varepsilon_r^e}{d\varepsilon_{\theta p} - d\varepsilon_\theta^e} = -\frac{\varsigma}{\beta} \tag{11}$$

where $\beta = (1+\sin\psi)/(1-\sin\psi)$, ψ is the dilation angle. ε^p_{rp} and $\varepsilon^p_{\theta p}$ are the radial and tangential plastic strain in plastic zone, ε_{rp} and $\varepsilon_{\theta p}$ the radial and tangential strains in plastic zone.

Based on Yu's (2002) the stress-strain relationship,

$$\left.\begin{aligned} d\varepsilon_r^e &= \frac{1-v^2(2-\varsigma)}{E}\left(d\sigma_r - \frac{\varsigma v}{1-v(2-\varsigma)}d\sigma_\theta\right) \\ d\varepsilon_\theta^e &= \frac{1-v^2(2-\varsigma)}{E}\left((1-v(\varsigma-1))d\sigma_\theta - \frac{v}{1-v(2-\varsigma)}d\sigma_r\right) \\ M &= \frac{E}{1-v^2(2-\varsigma)} \end{aligned}\right\} \tag{12}$$

Combining Eqs. (12) and (11),

$$\begin{aligned} \beta d\varepsilon_r + d\varepsilon_\theta &= \frac{1-v^2(2-\varsigma)}{E}\left[\beta - \frac{\varsigma v}{1-v(2-\varsigma)}\right]d\sigma_r \\ &+ \frac{1-v^2(2-\varsigma)}{E}\left[\varsigma(1-2v)+2v-\frac{\varsigma\beta v}{1-v(2-\varsigma)}\right]d\sigma_\theta \\ &= \frac{1}{M}\left[\beta - \frac{\varsigma v}{1-v(2-\varsigma)}\right]d\sigma_r \\ &+ \frac{1}{M}\left[\varsigma(1-2v)+2v-\frac{\varsigma\beta v}{1-v(2-\varsigma)}\right]d\sigma_\theta \end{aligned} \tag{13}$$

According to the yield Eq. (10), $d\sigma_\theta = \frac{1}{R}d\sigma_r$ can be obtained, the Eq. (13) can be derived,

$$d\varepsilon_r + \frac{\varsigma}{\beta}d\varepsilon_\theta = \frac{\xi}{\beta}d\sigma_r \tag{14}$$

$$\xi = \frac{1}{M}\left[\begin{aligned} &\left(\beta - \frac{\varsigma v}{1-v(2-\varsigma)}\right) \\ &+ \frac{((2(1+b)-mb)(1-\sin\varphi))}{M\left[2(1+b)(1+\sin\varphi)+mb(\sin\varphi-1)\right]} \\ &\left(\varsigma(1-2v)+2v-\frac{\varsigma\beta v}{1-v(2-\varsigma)}\right) \end{aligned}\right] \tag{15}$$

Following Yu and Carter (2002), and the relative velocity V is defined. The radius has a slight increment dr_p, and then the corresponding displacement of a particle of the cavity is du, $du=dr=Vdr_p$, u is a function of the current radius r and the radius of the plastic zone (r_p), that is, $u=(r, r_p)$, r_p and $r$are two independent variables, and the total differential is obtained,

$$\begin{aligned} du &= \left(\partial u/\partial r_p\right)dr_p + \left(\partial u/\partial r\right)dr \\ &= \left(\partial u/\partial r_p\right)dr_p + V\left(\partial u/\partial r\right)dr_p \end{aligned} \tag{16}$$

The particle velocity can be written,

$$V = \left(\partial u/\partial r_p\right)\Big/\left(1-\partial u/\partial r\right) \tag{17}$$

Follow a given material element and therefore,

$$\left\{\begin{aligned} d\varepsilon_r &= -\partial(du)/\partial r = -\left(\partial V/\partial r\right)dr_p \\ d\varepsilon_\theta &= -du/r = -\left(Vdr_p\right)/r \\ d\sigma_r &= \left(\left(\partial\sigma_r/\partial r_p\right)+V\left(\partial\sigma_r/\partial r\right)\right)dr_p \\ d\sigma_\theta &= \left(\left(\partial\sigma_\theta/\partial r_p\right)+V\left(\partial\sigma_\theta/\partial r\right)\right)dr_p \end{aligned}\right. \tag{18}$$

The Eq. (14) can also be obtained,

$$\frac{\partial V}{\partial r} + \frac{\varsigma V}{\beta r} = -\frac{\xi}{\beta}\left(\frac{\partial\sigma_r}{\partial r_p} + V\frac{\partial\sigma_r}{\partial r}\right) \tag{19}$$

Therefore,

$$\frac{\partial V}{\partial r} + P(r)V = Q(r) \tag{20}$$

where,

$$P(r) = \frac{\varsigma}{\beta r} - \frac{\xi q\varsigma(4(1+b)\sin\varphi)}{R\beta r\left(2(1+b)(1+\sin\varphi)+mb(\sin\varphi-1)\right)}\left(\frac{r_p}{r}\right)^{\varsigma\frac{4(1+b)\sin\varphi}{2(1+b)(1+\sin\varphi)+mb(\sin\varphi-1)}} \tag{21}$$

$$Q(r) = -\frac{s}{r_P}\left(\frac{r_P}{r}\right)^{\varsigma\frac{4(1+b)\sin\varphi}{2(1+b)(1+\sin\varphi)+mb(\sin\varphi-1)}} \tag{22}$$

$$q = \sigma_{rp} + \frac{[2(1+b)-mb](1-\sin\varphi)}{4(1+b)\sin\varphi}\sigma_0 \tag{23}$$

$$s = \frac{\xi q\varsigma(4(1+b)\sin\varphi)}{\beta\left(2(1+b)(1+\sin\varphi)+mb(\sin\varphi-1)\right)} \tag{24}$$

According to Eq. (7),

$$\left.\begin{aligned} V_{r=r_b} &= \delta(1+\varsigma) \\ \delta &= \frac{\left(\sigma_{rp}-\sigma_{h0}\right)}{2\varsigma G} \end{aligned}\right\} \tag{25}$$

The Eq. (20) can also be derived,

$$\begin{aligned} V = \exp&\left[-\frac{\xi q}{\beta}\left(\frac{r_p}{r}\right)^{\varsigma\frac{4(1+b)\sin\varphi}{2(1+b)(1+\sin\varphi)+mb(\sin\varphi-1)}}\right] \\ &\left\{\begin{aligned} &\sum_{n=0}^{\infty}H_n\left(\frac{r_p}{r}\right)^{\frac{\varsigma(4(1+b)\sin\varphi)(1+n)}{2(1+b)(1+\sin\varphi)+mb(\sin\varphi-1)}-1} \\ &+\left[\delta(\varsigma+1)\exp\left(\frac{\xi q}{\beta}\right)-\sum_{n=0}^{\infty}H_n\right]\left(\frac{r_p}{r}\right)^{\frac{\varsigma}{\beta}} \end{aligned}\right\} \end{aligned} \tag{26}$$

where,

$$H_n = \frac{1}{n!}\left(\frac{\xi q}{\beta}\right)^n \frac{\left(2(1+b)(1+\sin\varphi)+mb(\sin\varphi-1)\right)\beta s}{\left[(\varsigma+\beta)\left(2(1+b)(1+\sin\varphi)+mb(\sin\varphi-1)\right)-\varsigma\beta(4(1+b)\sin\varphi)(1+n)\right]} \tag{27}$$

For the cavity wall $r=a$, $V=da/dr_p$, so,

$$\begin{aligned} \frac{da}{dr_p} = \exp&\left[-\frac{\xi q}{\beta}\left(\frac{r_p}{r}\right)^{\varsigma\frac{4(1+b)\sin\varphi}{2(1+b)(1+\sin\varphi)+mb(\sin\varphi-1)}}\right] \\ &\left\{\begin{aligned} &\sum_{n=0}^{\infty}H_n\left(\frac{r_p}{r}\right)^{\frac{(4(1+b)\sin\varphi)\varsigma(1+n)}{2(1+b)(1+\sin\varphi)+mb(\sin\varphi-1)}-1} \\ &+\left[\delta(\varsigma+1)\exp\left(\frac{\xi q}{\beta}\right)-\sum_{n=0}^{\infty}H_n\right]\left(\frac{r_p}{r}\right)^{\frac{\varsigma}{\beta}} \end{aligned}\right\} \end{aligned} \tag{28}$$

According to the similarity solutions, the geometrically similar in the plastic zone can be obtained,

$$\frac{da}{dr_p} = \frac{a}{r_p} \tag{29}$$

The ratio of the radius (r_p) to the radius of cavity (a) can be obtained,

$$\frac{a}{r_p} = \exp\left[-\frac{\xi q}{\beta}\left(\frac{r_p}{r}\right)^{\varsigma\frac{4(1+b)\sin\varphi}{2(1+b)(1+\sin\varphi)+mb(\sin\varphi-1)}}\right] \cdot \left\{ \begin{aligned} &\sum_{n=0}^{\infty} H_n\left(\frac{r_p}{r}\right)^{\frac{(4(1+b)\sin\varphi)\varsigma(1+n)}{2(1+b)(1+\sin\varphi)+mb(\sin\varphi-1)}-1} \\ &+\left[\delta(\varsigma+1)\exp\left(\frac{\xi q}{\beta}\right)-\sum_{n=0}^{\infty}H_n\right]\left(\frac{r_p}{r}\right)^{\frac{\varsigma}{\beta}} \end{aligned} \right\} \tag{30}$$

Once a is determined, the radius of the plastic zone (r_p) can be easily obtained.

The finite initial radius (a_0) problem response is consistent with the created problem response in the region $r \geq a_0$, the equations can be obtained (Zhou *et al.* 2018),

$$\ln\left(\frac{a}{a_0}\right) = \ln(\eta) + \int_1^{\eta} \frac{d\eta}{\bar{w}(\eta)-1} \tag{31}$$

$$\eta = \frac{a}{r_p} \tag{32}$$

where η is a dimensionless ratio, $\bar{w}$ is the dimension radial velocity, $\bar{w}(\eta)$ takes the following approximate form (Russell and Khalili 2002),

$$\bar{w}_p = \frac{s_u}{2G} \tag{33}$$

$$\bar{w}(\eta) = \bar{w}_p h_1 \eta^{-h_2} \tag{34}$$

where h_1 and h_2 are related to the initial condition, h_1 is approximately equal to 1, and h_2 varying from 0.7 ζ to ζ, $h_2 \approx \zeta$ is assumed to the following calculation in the study.

Combining Eqs. (33) and (34), the Eq. (31) can be derived,

$$\ln\left(\frac{a}{a_0}\right) = \ln(\eta) - \frac{\ln(-h_1\bar{w}_p + \eta^{1+h_2}) - \ln(-h_1\bar{w}_p + 1)}{1+h_2} \tag{35}$$

2.5 Plastic zone

2.5.1 The total radial and tangential stress in plastic zone

Combining Eqs. (5), (6) and (1), the following equations can also be obtained considering the boundary conditions,

$$\sigma_{rp} = \frac{(\varsigma+1)R\sigma_{h0} + \varsigma\sigma_0}{R+\varsigma} \tag{36}$$

$$\sigma_{\theta p} = \frac{(\varsigma+1)\sigma_{h0} - \sigma_0}{R+\varsigma} \tag{37}$$

Because the soil mass satisfies the stress yield criterion and the equilibrium equation in the plastic zone, so, combining Eqs. (4) and (1),

$$\sigma_r = K\left(\frac{1}{r}\right)^{\varsigma\frac{R-1}{R}} + \frac{\sigma_0}{1-R} \tag{38}$$

Combining Eqs. (38), (36) and (9),

$$K = \left(\frac{(\varsigma+1)R\sigma_{h0} + \varsigma\sigma_0}{R+\varsigma} - \frac{\sigma_0}{1-R}\right) r_p^{\varsigma\frac{R-1}{R}} \tag{39}$$

The total radial stress can be written,

$$\sigma_r = \left(\frac{(\varsigma+1)R\sigma_{h0} + \varsigma\sigma_0}{R+\varsigma} - \frac{\sigma_0}{1-R}\right)\left(\frac{r_p}{r}\right)^{\varsigma\frac{R-1}{R}} + \frac{\sigma_0}{1-R} \tag{40}$$

So, combining Eq. (40), and (1), the tangential stress can be obtained,

$$\sigma_\theta = \frac{1}{R}\left[\begin{aligned} &\left(\frac{(\varsigma+1)R\sigma_{h0} + \varsigma\sigma_0}{R+\varsigma} - \frac{\sigma_0}{1-R}\right)\left(\frac{r_p}{r}\right)^{\varsigma\frac{R-1}{R}} \\ &+\frac{R\sigma_0}{1-R} \end{aligned}\right] \tag{41}$$

2.5.2 Limit expanding pressure in plastic zone

According to the Eq. (40) the limit expanding pressure can be derived,

$$\sigma_r(r = a_u) = p_u \tag{42}$$

$$p_u = \left(\sigma_{rp} + \frac{\sigma_0}{R-1}\right)\left(\frac{r_p}{a_u}\right)^{\varsigma\frac{R-1}{R}} - \frac{\sigma_0}{R-1} \tag{43}$$

3. Validation and discussions

Yu and Carter (2002) is presented to verify the suitability of the presented theoretical solution. The value of the model parameters chosen are, σ_{h0}=100 kPa, c/σ_{h0}=1, $2G_0/\sigma_{h0}$=20, the Poisson's ratio ν =0.3, following Yu and Carter (2002), the internal friction angle is φ with varying from 20 to 50 degrees, and the dilation angle is ψ with varying from 0 to φ degrees, respectively. The presented procedure is programmed into a Matlab code, the above code can be solved through Matlab using the Levenberg-Marquardt algorithm conveniently. As shown in Tables 1 and 3, it is shown that the results of Yu and Carter (2002) are approximately equal to the presented solution, the comparison between the presented solution and the data from Yu and Carter (2002) are carried out and practically identical.

As shown in Tables 2 and 4. The influence of initial stress anisotropy coefficient b on the radius ratio and normalized internal pressure are investigated, the radius ratio (r_p/a) decreases nonlinearly with the increase of initial stress anisotropy coefficient b, and the normalized internal pressure (p/σ_{h0}) increases nonlinearly with the increase of

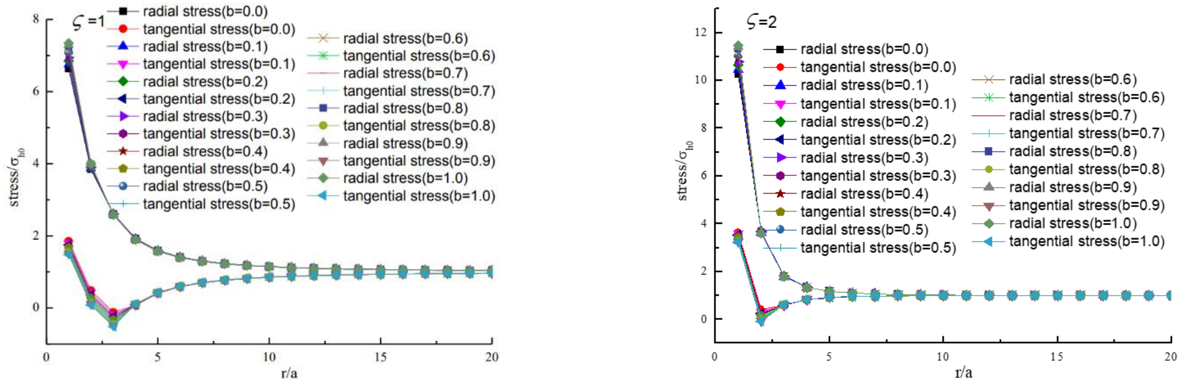

(a) (b)

Fig. 2 Influence of initial stress anisotropy coefficient b on the stress, (a) ζ=1 and (b) ζ=2

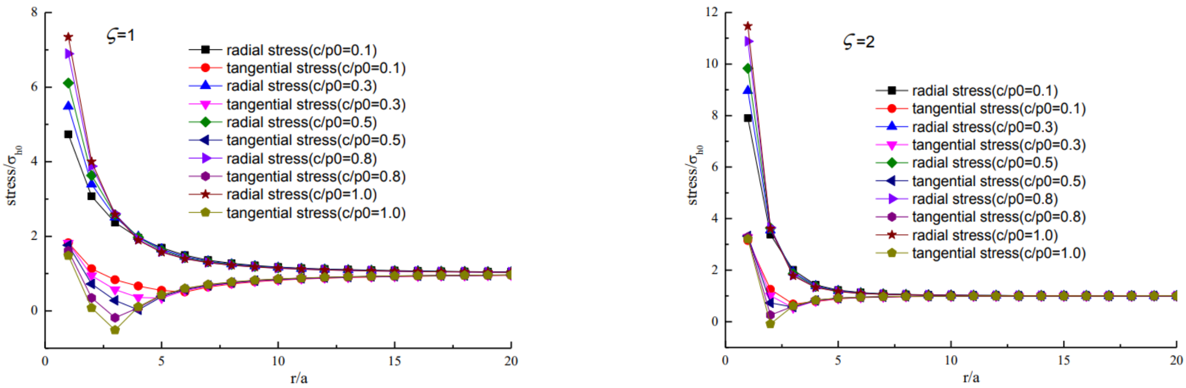

(a) (b)

Fig. 3 Influence of cohesion (C) on the stress, (a) ζ=1 and (b) ζ=2

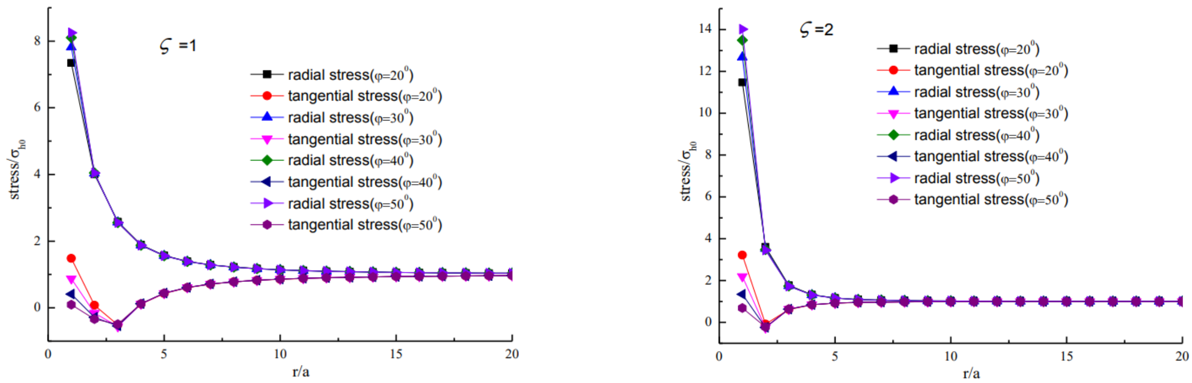

(a) (b)

Fig. 4 Influence of the internal friction angle (φ) on the stress, (a) ζ=1 and (b) ζ=2

initial stress anisotropy coefficient b, it is indicate that ignoring the influence of initial stress anisotropy coefficient b on the radius ratio and normalized internal pressure will be miscalculated results.

The displacement analysis of cavity expansion problem is often used for calculating the lateral displacement caused by installing columns (pile). For example, static pressure pile are widely used in urban construction due to low construction noise, no vibration, and quick construction. However, the static pressure pile belongs to the displacement-pile. During the piling process, the soil around the pile is laterally moved due to the cavity expansion, which will adversely affect the adjacent buildings (structures) and municipal pipelines (Zhang and Li 2015). As shown in above displacement analysis, it also proves that the initial stress anisotropy effect of the soil around pile is neglected to provide a conservative evaluation in Chai's study (Chai *et al.* 2009).

The value of the model parameters chosen are, σ_{h0}=100 kPa, c/σ_{h0}=1, $2G_0/\sigma_{h0}$=20, the Poisson's ratio of soil mass v =0.3, φ=20, ψ =20.

As shown in Fig. 2, the influence of the initial stress anisotropy coefficient b on the normalized stress are investigated, the influence of the initial stress anisotropy

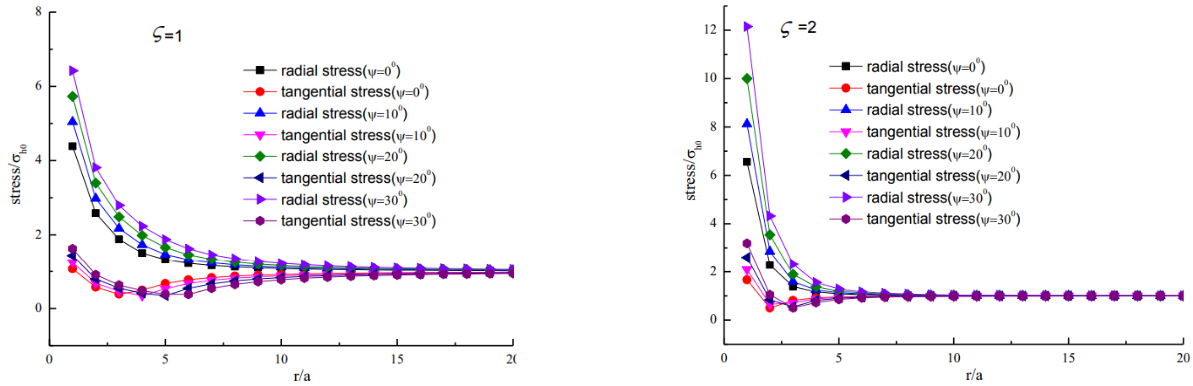

(a) (b)

Fig. 5 Influence of the dilation angle (ψ) on the stress, (a) ζ,=1 and (b) ζ=2

coefficient b on the stress are not obvious, the tangential stress are the minimum value around EP boundary. The change of the stress for ζ =2 are more obvious than that for ζ =1.

The stress analysis be applied to interpret and predict the stress field around the pile shaft on the pile-installation tests in saturated soil mass (Randolph, 2003). As shown in above stress analysis, it also proves that the initial stress anisotropy effect of the soil around pile is neglected to provide a nonconservative evaluation for study.

The value of the model parameters chosen are, σ_{h0}=100 kPa, $2G_0/\sigma_{h0}$=20, the Poisson's ratio of soil mass, v =0.3, φ=20, ψ =20, b=1.0, c/σ_{h0}= 0.1, 0.3, 0.5, 0.8 and 1.0.

As shown in Fig. 3. The influence of the cohesion (c) on the normalized stress are investigated, the influence of the cohesion (c) on the stress are obvious in the plastic zone, the radial stress increases nonlinearly with the increase of cohesion (c) and the tangential stress decreases nonlinearly with the increase of cohesion (c), the change of the stress are more obvious for ζ =1 than that for ζ =2. It is indicate that ignoring the influence of cohesion (c) on the stress of the plastic zone will be miscalculated results.

The value of the model parameters chosen are, σ_{h0}=100 kPa, c/σ_{h0}= 1, $2G_0/\sigma_{h0}$=20, the Poisson's ratio of soil mass v =0.3, ψ =20, b=1.0, φ=20, 30, 40 and 50.

As shown in Fig. 4. The influence of the internal friction angle (φ) on the normalized stress are investigated, the influence of the internal friction angle (φ) on the stress are not obvious in the plastic zone than that the influence of the cohesion (c). The radial stress increases nonlinearly with the increase of internal friction angle (φ) and the tangential stress decreases nonlinearly with the increase of internal friction angle (φ), this trend is similar to that in Fig. 3. The change of the stress are more obvious for ζ =1 than that for ζ =2. It is indicate that ignoring the influence of internal friction angle (φ) on the stress of the plastic zone will be miscalculated results.

The value of the model parameters chosen are, σ_{h0}=100 kPa, c/σ_{h0}=0.1, $2G_0/\sigma_{h0}$=20, the Poisson's ratio of soil mass, v =0.3, φ=30, b=1.0, , ψ =0, 10, 20 and 30.

As shown in Fig. 5. The influence of the dilation angle (ψ) on the normalized stress is investigated, the influence of the dilation angle (ψ) on the stress is obvious in the plastic zone than that the influence of the cohesion (c) and internal friction angle (φ). The radial stress increases nonlinearly with the increase of the dilation angle (ψ), and the tangential stress increases nonlinearly with the increase of the dilation angle (ψ), this trend is different to that in Fig. 3 and Fig. 4. The change of the stress are more obvious for ζ =1 than that for ζ =2. It is indicate that ignoring the influence of the dilation angle (ψ) on the stress of the plastic zone will be miscalculated results.

4. Conclusions

A novel theoretical solution is proposed for drained cavity expansion on the basis of unified strength failure criterion, and considers the influence of initial stress anisotropy. Compared with the previous similarity solution, the following improvements have been achieved:

(1) A more advanced soil mass model (UST model) is introduced into analyze the cavity expansion mechanisms, and it reflects the influence of the intermediate principal stress on the yielding of geomaterial;

(2) A more advanced Levenberg-Marquardt algorithm is introduced into calculate the radius and stress in this study, and the comparison between the presented solution and the previous similarity solution is carried out and shows more accurate;

(3) The influence of initial stress anisotropy on the radius ratio and normalized internal pressure are investigated, the radius ratio decreases nonlinearly with the increase of initial stress anisotropy coefficient b, and the normalized internal pressure increases nonlinearly with the increase of initial stress anisotropy coefficient b.

(4) The influence of the initial stress anisotropy on the normalized stress are investigated, the influence of the initial stress anisotropy coefficient b on the stress are not obvious, and the tangential stress reach the minimum value around EP boundary. The change of the stress for ζ =2 are more obvious than that for ζ =1.

Acknowledgments

This work was supported by the National Key R&D Program of China (2017YFB1201204). The first author thanks

Project 2018zzts188 supported by Innovation Foundation for Postgraduate of the Central South University. The editor's and anonymous reviewer's comments have improved the quality of the study and are also greatly acknowledged.

References

Andersen, K.H. (1980), "Cyclic and static laboratory tests on Drammen clay", *J. Soil Mech. Found. Div.*, **106**(5), 499-529.

Carter, J.P. Booker, J.R. and Yeung, S.K. (1986), "Cavity expansion in cohesive frictional soils", *Géotechnique*, **36**(3), 345-358. https://doi.org/10.1680/geot.1986.36.3.349.

Carter, J.P., Randolph, M.F. and Wroth, C.P. (1979), "Stress and pore pressure changes in clay during and after the expansion of a cylindrical cavity", *Int. J. Numer. Anal. Meth. Geomech.*, **3**(4), 305-322. https://doi.org/10.1002/nag.1610030402.

Chai, J., Carter, J. P., Miura, N. and Zhu, H. (2009), "Improved prediction of lateral deformations due to installation of soil-cement columns", *J. Geotech. Geoenviron. Eng.*, **135**(12), 1836-1845. https://doi.org/10.1061/(ASCE)GT.1943-5606.0000155.

Chen, S.L. and Abousleiman, Y.N. (2013), "Exact drained solution for cylindrical cavity expansion in modified cam clay soil", *Géotechnique,* **63**(6), 510-517. https://doi.org/10.1680/geot.11.P.088.

Chen, G.H., Zou, J.F. and Chen, J.Q. (2019a), "Shallow tunnel face stability considering pore water pressure in non-homogeneous and anisotropic soils", *Comput. Geotech.*, **116**, 103205. https://doi.org/10.1016/j.compgeo.2019.103205.

Chen, G.H., Zou, J.F. and Qian, Z.H. (2019b). "An improved collapse analysis mechanism for the face stability of shield tunnel in layered soils", *Geomech. Eng.*, **17**(1), 97-107. https://doi.org/10.12989/gae.2019.17.1.097.

Collins, I.F. and Yu, H.S. (1996), "Undrained cavity expansions in critical state soils", *Int. J. Numer. Anal. Meth. Geomech.*, **20**(7), 489-516. https://doi.org/10.1002/(SICI)1096-9853(199607)20:7%3C489::AID-NAG829%3E3.0.CO;2-V.

Hill, R. (1950), *The Mathematical Theory of Plasticity*, Clarendon Press.

Li, L., Li, J. and Sun, D. (2016), "Anisotropically elasto-plastic solution to undrained cylindrical cavity expansion in K0-consolidated clay", *Comput. Geotech.*, **73**, 83-90. https://doi.org/10.1016/j.compgeo.2015.11.022.

Li, C., Zou, J.F. and A, S.G. (2019a), "Closed-form solution for undrained cavity expansion in anisotropic soil mass based on the spatially mobilized plane failure criterion", *Int. J. Geomech.*, **19**(7), 04019075. https://doi.org/10.1061/(ASCE)GM.1943-5622.0001458.

Li, C., Zou, J.F. and Zhou, H. (2019b), "Cavity expansions in k0 consolidated clay", *Eur. J. Environ. Civ. Eng.*, 1-19. https://doi.org/10.1080/19648189.2019.1605937.

Marchi, M., Gottardi, G. and Soga, K. (2014), "Fracturing pressure in clay", *J. Geotech. Geoenviron. Eng.*, **140**(2), 04013008. https://doi.org/10.1061/(ASCE)GT.1943-5606.0001019.

Mo, P.Q., Marshall, A.M. and Yu, H.S. (2016), "Interpretation of cone penetration test data in layered soils using cavity expansion analysis", *J. Geotech. Geoenviron. Eng.*, **143**(1), 04016084. https://doi.org/10.1061/(ASCE)GT.1943-5606.0001577.

Mo, P.Q. and Yu, H.S. (2016), "Undrained cavity-contraction analysis for prediction of soil behavior around tunnels", *Int. J. Geomech.*, **17**(5), 04016121. https://doi.org/10.1061/(ASCE)GM.1943-5622.0000816.

Mo, P.Q. and Yu, H.S. (2017a), "Undrained cavity expansion analysis with a unified state parameter model for clay and sand", *Géotechnique,* **67**(6), 503-515. https://doi.org/10.1680/jgeot.15.P.261.

Mo, P.Q. and Yu, H.S. (2017b), "Drained cavity expansion analysis with a unified state parameter model for clay and sand", *Can. Geotech. J.*, **55**(7), 1029-1040. https://doi.org/10.1139/cgj-2016-0695.

Park, K.H., Tontavanich, B. and Lee, J.G. (2008), "A simple procedure for ground response curve of circular tunnel in elastic-strain softening rock masses", *Tunn. Undergr. Sp. Technol.*, **23**(2), 151-159. https://doi.org/10.1016/j.tust.2007.03.002.

Peng, X., Yu, P., Zhang, Y. and Chen, G. (2018), "Applying modified discontinuous deformation analysis to assess the dynamic response of sites containing discontinuities", *Eng. Geol.*, **246**, 349-360. https://doi.org/10.1016/j.enggeo.2018.10.011.

Randolph, M.F. (2003), "Science and empiricism in pile foundation design", *Géotechnique,* **53**(10), 847-876. https://doi.org/10.1680/geot.2003.53.10.847.

Russell, A.R. and Khalili, N. (2002), "Drained cavity expansion in sands exhibiting particle crushing", *Int. J. Numer. Anal. Meth. Geomech.,* **26**(4), 323-340. https://doi.org/10.1002/nag.203.

Salgado, R. and Prezzi, M. (2007), "Computation of cavity expansion pressure and penetration resistance in sands", *Int. J. Geomech.*, **7**, 251-265. https://doi.org/10.1061/(ASCE)1532-3641(2007)7:4(251).

Seo, H.J., Jeong, K.H., Choi, H. and Lee, I.M. (2012), "Pullout Resistance Increase of Soil Nailing Induced by Pressurized Grouting", *J. Geotech. Geoenviron. Eng.*, **138**(5), 604-613. https://doi.org/10.1061/(ASCE)GT.1943-5606.0000622.

Silvestri, V. and Abou-Samra, G. (2012), "Analytical solution for undrained plane strain expansion of a cylindrical cavity in modified Cam clay", *Geomech. Eng.*, **4**(1), 19-37. https://doi.org/10.12989/gae.2012.4.1.019.

Teh, C.I. and Houlsby, G.T. (1991), "Analytical study of the cone penetration test in clay", *Geotechnique,* **41**(1), 17-34. https://doi.org/10.1680/geot.1991.41.1.17.

Tolooiyan, A. and Gavin, K. (2011), "Modelling the cone penetration test in sand using cavity expansion and arbitrary Lagrangian Eulerian finite element methods", *Comput. Geotech.*, **38**(4), 482-490. https://doi.org/10.1016/j.compgeo.2011.02.012.

Vesic, A.S. (1972), "Expansion of cavities in infinite soil mass", *J. Soil Mech. Found. Div.*, **98**(3), 265-290.

Wang, S., Wu, Z., Guo, M. and Ge, X. (2012), "Theoretical solutions of a circular tunnel with the influence of axial in situ stress in elastic–brittle–plastic rock", *Tunn. Undergr. Sp. Technol.*, **30**, 155-168. https://doi.org/10.1016/j.tust.2012.02.016.

Wang, S. and Yin, S. (2011), "A closed-form solution for a spherical cavity in the elastic-brittle-plastic medium", *Tunn. Undergr. Sp. Technol.*, **26**(1), 236-241. https://doi.org/10.1016/j.tust.2010.06.005.

Xiao, Y., Sun, Y., Yin, F., Liu, H. and Xiang, J. (2016), "Constitutive modeling for transparent granular soils", *Int. J. Geomech.*, 04016150. https://doi.org/10.1061/(ASCE)GM.1943-5622.0000857.

Yang, X.L. and Pan, Q.J. (2015), "Three dimensional seismic and static stability of rock slopes", *Geomech. Eng.*, **8**(1), 97-111. http://dx.doi.org/10.12989/gae.2015.8.1.097.

Yu, H.S. (2000), *Cavity Expansion Methods in Geomechanics*, Kluwer Academic Publishers.

Yu, H.S. and Carter, J.P. (2002), "Rigorous similarity solutions for cavity expansion in cohesive-frictional soils", *Int. J. Geomech.*, **2**(2), 233-258. https://doi.org/10.1061/(ASCE)1532-3641(2002)2:2(233).

Yu, M.H. (2004), *Unified Strength Theory and Applications*, Springer-Verlag.

Zhang, Y., Chen, G., Zheng, L., Li, Y. and Wu, J. (2013), "Effects of near-fault seismic loadings on run-out of large-scale landslide: a case study", *Eng*. *Geol*., **166**(8), 216-236. https://doi.org/10.1016/j.enggeo.2013.08.002.

Zhang, Y.G. and Li, J.P. (2015), "Lateral displacements of ground caused by piles installation in soft clay", *J. Tongji Univ*. *Nat*. *Sci*., **43**(12), 1801-1806 (in Chinese).

Zhang, Y., Wang, J., Xu, Q., Chen, G., Zhao, J.X., Zheng, L. and Yu, P. (2015a), "DDA validation of the mobility of earthquake-induced landslides", *Eng*. *Geol*., **194**(26), 38-51. https://doi.org/10.1016/j.enggeo.2014.08.024.

Zhang, Y., Zhang, J., Chen, G., Zheng, L. and Li, Y. (2015b), "Effects of vertical seismic force on initiation of the Daguangbao landslide induced by the 2008 Wenchuan earthquake", *Soil Dyn*. *Earthq*. *Eng*., **73**, 91-102. https://doi.org/10.1016/j.soildyn.2014.06.036.

Zhao, L.H., Cheng, X., Li, D.J. and Zhang, Y.B. (2019), "Influence of non-dimensional strength parameters on the seismic stability of cracked slopes", *J. Mount*. *Sci*., **16**(1), 153-167. https://doi.org/10.1007/s11629-017-4753-9.

Zhou, H., Kong, G., Liu, H. and Laloui, L. (2018), "Similarity solution for cavity expansion in thermoplastic soil", *Int*. *J*. *Numer*. *Anal*. *Meth*. *Geomech*., **42**(2), 274-294. https://doi.org/10.1002/nag.2724.

Zhou, H., Liu, H., Randolph, M.F., Kong, G. and Cao, Z. 2017), "Experimental and analytical study of X-section cast-in-place concrete pile installation influence", *Int*. *J*. *Phys*. *Modell*. *Geotech*., **17**(2), 1-19. https://doi.org/10.1680/jphmg.15.00037.

Zou, J.F., Chen, G. and Qian, Z. (2019), "Tunnel face stability in cohesion-frictional soils considering the soil arching effect by improved failure models", *Comput*. *Geotech*., **106**, 1-17. https://doi.org/10.1016/j.compgeo.2018.10.014.

Zou, J.F., Chen, K.F. and Pan, Q.J. (2017), "Influences of seepage force and out-of-plane stress on cavity contracting and tunnel opening", *Geomech*. *Eng*., **13**(6), 907-928. https://doi.org/10.12989/gae.2017.13.6.907.

Zou, J.F. and Wei, X.X. (2018), "An improved radius-incremental-approach of stress and displacement for strain-softening surrounding rock considering hydraulic-mechanical coupling", *Geomech*. *Eng*., **16**(1), 59-69. https://doi.org/10.12989/gae.2018.16.1.059.

Zou, J.F., Wei, A. and Yang, T. (2018), "Elasto-plastic solution for shallow tunnel in semi-infinite space", *Appl*. *Math*. *Modell.,* **64**(12), 669-687. https://doi.org/10.1016/j.apm.2018.07.049.

Zou, J.F. and Zhang, P.H. (2019), "Analytical model of fully grouted bolts in pull-out tests and in situ rock masses", *Int*. *J*. *Rock Mech*. *Min*. *Sci*., **113**(1), 278-294. https://doi.org/10.1016/j.ijrmms.2018.11.015.

GC

Appendix

Table 1 The comparison between the presented results (r_p/a) and Yu and Carter (2002)

b	φ(°)	ψ (°)	r_p/a, ζ=1 Yu and Carter (2002)	r_p/a, ζ=1 the presented solution	Error (%)	r_p/a, ζ=2 Yu and Carter (2000)	r_p/a, ζ=2 the presented solution	Error (%)
0.0	20	0	2.55	2.5542	0.16%	1.77	1.7663	-0.21%
		10	2.96	2.9594	-0.02%	1.99	1.9931	0.16%
		20	3.40	3.3988	-0.04%	2.26	2.2564	-0.16%
	30	0	2.49	2.4929	0.12%	1.71	1.7140	0.23%
		10	2.86	2.8618	0.06%	1.91	1.9094	-0.03%
		20	3.25	3.2531	0.10%	2.13	2.1274	-0.12%
		30	3.65	3.6507	0.02%	2.36	2.3606	0.03%
	40	0	2.47	2.4677	-0.09%	1.68	1.6784	-0.10%
		10	2.82	2.8164	-0.13%	1.85	1.8529	0.16%
		20	3.18	3.1805	0.02%	2.04	2.0418	0.09%
		30	3.54	3.5444	0.12%	2.24	2.2375	-0.11%
		40	3.89	3.8910	0.03%	2.43	2.4301	0.00%
	50	0	2.48	2.4754	-0.19%	1.66	1.6589	-0.07%
		10	2.82	2.8171	-0.10%	1.82	1.8206	0.03%
		20	3.17	3.1698	-0.01%	1.99	1.9919	0.10%
		30	3.52	3.5183	-0.05%	2.17	2.1654	-0.21%
		40	3.85	3.8467	-0.09%	2.33	2.3322	0.09%
		50	4.14	4.1392	-0.02%	2.48	2.4835	0.14%

Table 2 The presented results (r_p/a) for different b

	φ(°)	ψ (°)	b=0.0	b=0.1	b=0.2	b=0.3	b=0.4	b=0.5	b=0.6	b=0.7	b=0.8	b=0.9	b=1.0
r_p/a, ζ=1	20	0	2.5542	2.5198	2.4907	2.4658	2.4442	2.4253	2.4087	2.3939	2.3806	2.3687	2.3579
		10	2.9594	2.9122	2.8725	2.8385	2.8091	2.7834	2.7608	2.7408	2.7228	2.7067	2.6921
		20	3.3988	3.3364	3.2839	3.2392	3.2006	3.1669	3.1373	3.1111	3.0877	3.0666	3.0476
	30	0	2.4929	2.4677	2.4464	2.4282	2.4125	2.3987	2.3867	2.3759	2.3664	2.3577	2.3500
		10	2.8618	2.8274	2.7986	2.7740	2.7527	2.7342	2.7180	2.7035	2.6907	2.6791	2.6687
		20	3.2531	3.2081	3.1704	3.1384	3.1107	3.0867	3.0656	3.0469	3.0302	3.0152	3.0017
		30	3.6507	3.5940	3.5466	3.5063	3.4716	3.4415	3.4151	3.3917	3.3709	3.3522	3.3354
	40	0	2.4677	2.4499	2.4350	2.4223	2.4113	2.4017	2.3934	2.3859	2.3793	2.3733	2.3679
		10	2.8164	2.7924	2.7723	2.7552	2.7405	2.7277	2.7164	2.7065	2.6976	2.6896	2.6824
		20	3.1805	3.1493	3.1233	3.1011	3.0821	3.0655	3.0510	3.0382	3.0267	3.0165	3.0072
		30	3.5444	3.5055	3.4729	3.4453	3.4216	3.4010	3.3830	3.3670	3.3528	3.3401	3.3286
		40	3.8910	3.8441	3.8050	3.7718	3.7433	3.7186	3.6970	3.6779	3.6609	3.6457	3.6320
	50	0	2.4754	2.4637	2.4540	2.4457	2.4386	2.4324	2.4269	2.4221	2.4178	2.4140	2.4105
		10	2.8171	2.8014	2.7884	2.7772	2.7677	2.7594	2.7521	2.7457	2.7399	2.7348	2.7301
		20	3.1698	3.1496	3.1327	3.1184	3.1060	3.0954	3.0860	3.0777	3.0703	3.0637	3.0578
		30	3.5183	3.4932	3.4722	3.4544	3.4392	3.4259	3.4143	3.4040	3.3949	3.3868	3.3794
		40	3.8467	3.8165	3.7914	3.7701	3.7519	3.7361	3.7222	3.7100	3.6991	3.6894	3.6806
		50	4.1392	4.1044	4.0754	4.0508	4.0298	4.0115	3.9955	3.9814	3.9689	3.9577	3.9476

Table 2 Continued

	φ(°)	ψ (°)	b=0.0	b=0.1	b=0.2	b=0.3	b=0.4	b=0.5	b=0.6	b=0.7	b=0.8	b=0.9	b=1.0
r_p/a, ζ=2	20	0	1.7663	1.7494	1.7350	1.7226	1.7119	1.7024	1.6940	1.6864	1.6797	1.6736	1.6681
		10	1.9931	1.9692	1.9489	1.9314	1.9162	1.9029	1.8911	1.8807	1.8713	1.8628	1.8551
		20	2.2564	2.2232	2.1951	2.1711	2.1503	2.1320	2.1160	2.1017	2.0889	2.0773	2.0669
	30	0	1.7140	1.7009	1.6898	1.6803	1.6720	1.6647	1.6583	1.6526	1.6474	1.6428	1.6386
		10	1.9094	1.8912	1.8758	1.8626	1.8512	1.8412	1.8324	1.8245	1.8175	1.8112	1.8054
		20	2.1274	2.1028	2.0821	2.0643	2.0490	2.0357	2.0239	2.0134	2.0041	1.9957	1.9881
		30	2.3606	2.3284	2.3013	2.2783	2.2584	2.2411	2.2259	2.2124	2.2003	2.1895	2.1798
	40	0	1.6784	1.6687	1.6605	1.6535	1.6474	1.6421	1.6374	1.6333	1.6295	1.6262	1.6231
		10	1.8529	1.8396	1.8285	1.8190	1.8108	1.8036	1.7972	1.7916	1.7866	1.7821	1.7780
		20	2.0418	2.0243	2.0096	1.9971	1.9863	1.9769	1.9686	1.9613	1.9547	1.9488	1.9435
		30	2.2375	2.2152	2.1964	2.1805	2.1668	2.1549	2.1444	2.1352	2.1269	2.1195	2.1128
		40	2.4301	2.4026	2.3796	2.3601	2.3433	2.3287	2.3159	2.3046	2.2946	2.2856	2.2774
	50	0	1.6589	1.6523	1.6467	1.6420	1.6379	1.6343	1.6311	1.6283	1.6258	1.6236	1.6215
		10	1.8206	1.8117	1.8043	1.7979	1.7924	1.7876	1.7834	1.7796	1.7763	1.7733	1.7706
		20	1.9919	1.9804	1.9707	1.9624	1.9553	1.9491	1.9437	1.9389	1.9346	1.9308	1.9273
		30	2.1654	2.1509	2.1387	2.1284	2.1195	2.1118	2.1051	2.0991	2.0938	2.0890	2.0847
		40	2.3322	2.3147	2.3000	2.2876	2.2769	2.2676	2.2595	2.2523	2.2460	2.2402	2.2351
		50	2.4835	2.4630	2.4460	2.4315	2.4191	2.4084	2.3989	2.3906	2.3832	2.3766	2.3707

Table 3 The comparison between the presented results (p/σ_{h0}) and Yu and Carter (2002)

b	φ(°)	ψ (°)	p/σ_{h0}, ζ=1 Yu and Carter (2002)	p/σ_{h0}, ζ=1 the presented solution	Error (%)	p/σ_{h0}, ζ=2 Yu and Carter (2000)	p/σ_{h0}, ζ=2 the presented solution	Error (%)
0.0	20	0	5.36	5.3635	0.07%	7.39	7.3896	-0.01%
		10	6.00	5.9957	-0.07%	8.72	8.7184	-0.02%
		20	6.64	6.6350	-0.08%	10.26	10.2643	0.04%
	30	0	5.80	5.8024	0.04%	8.36	8.3553	-0.06%
		10	6.53	6.5283	-0.03%	9.92	9.9168	-0.03%
		20	7.27	7.2651	-0.07%	11.72	11.7227	0.02%
		30	7.98	7.9841	0.05%	13.72	13.7245	0.03%
	40	0	6.11	6.1089	-0.02%	9.11	9.1140	0.04%
		10	6.90	6.9045	0.07%	10.84	10.8391	-0.01%
		20	7.71	7.7125	0.03%	12.81	12.8133	0.03%
		30	8.50	8.5003	0.00%	14.97	14.9703	0.00%
		40	9.23	9.2345	0.05%	17.20	17.2000	0.00%
	50	0	6.29	6.2911	0.02%	9.66	9.6581	-0.02%
		10	7.14	7.1375	-0.04%	11.50	11.4963	-0.03%
		20	8.00	7.9971	-0.04%	13.58	13.5791	-0.01%
		30	8.83	8.8341	0.05%	15.83	15.8262	-0.02%
		40	9.61	9.6124	0.02%	18.12	18.1167	-0.02%
		50	10.30	10.2986	-0.01%	20.30	20.3005	0.00%

Table 4 The presented results (p/σ_{h0}) for different b

	φ(°)	ψ (°)	b=0.0	b=0.1	b=0.2	b=0.3	b=0.4	b=0.5	b=0.6	b=0.7	b=0.8	b=0.9	b=1.0
p/σ_{h0}, ζ=1	20	0	5.3635	5.4586	5.5412	5.6135	5.6775	5.7344	5.7854	5.8314	5.8729	5.9108	5.9454
		10	5.9957	6.1018	6.1937	6.2741	6.3451	6.4082	6.4646	6.5154	6.5613	6.6031	6.6412
		20	6.6350	6.7519	6.8530	6.9413	7.0191	7.0882	7.1500	7.2054	7.2556	7.3011	7.3426
	30	0	5.8024	5.8796	5.9458	6.0033	6.0536	6.0980	6.1375	6.1729	6.2047	6.2335	6.2597
		10	6.5283	6.6142	6.6877	6.7513	6.8070	6.8561	6.8996	6.9386	6.9737	7.0054	7.0342
		20	7.2651	7.3592	7.4397	7.5092	7.5700	7.6235	7.6709	7.7133	7.7514	7.7858	7.8170
		30	7.9841	8.0858	8.1726	8.2475	8.3129	8.3703	8.4213	8.4667	8.5075	8.5444	8.5778
	40	0	6.1089	6.1659	6.2144	6.2561	6.2923	6.3241	6.3523	6.3773	6.3998	6.4201	6.4384
		10	6.9045	6.9677	7.0212	7.0673	7.1072	7.1423	7.1732	7.2008	7.2255	7.2477	7.2678
		20	7.7125	7.7814	7.8397	7.8897	7.9331	7.9712	8.0047	8.0345	8.0612	8.0853	8.1070
		30	8.5003	8.5742	8.6367	8.6903	8.7367	8.7773	8.8131	8.8449	8.8734	8.8990	8.9222
		40	9.2345	9.3127	9.3787	9.4352	9.4841	9.5269	9.5646	9.5980	9.6279	9.6548	9.6792
	50	0	6.2911	6.3290	6.3610	6.3883	6.4120	6.4326	6.4508	6.4670	6.4814	6.4944	6.5061
		10	7.1375	7.1794	7.2147	7.2448	7.2708	7.2936	7.3136	7.3313	7.3471	7.3614	7.3742
		20	7.9971	8.0425	8.0808	8.1135	8.1416	8.1662	8.1878	8.2070	8.2241	8.2395	8.2534
		30	8.8341	8.8826	8.9234	8.9582	8.9882	9.0144	9.0374	9.0578	9.0759	9.0923	9.1070
		40	9.6124	9.6635	9.7064	9.7429	9.7744	9.8018	9.8259	9.8473	9.8663	9.8834	9.8988
		50	10.2986	10.3516	10.3961	10.4339	10.4665	10.4949	10.5199	10.5419	10.5616	10.5793	10.5952
p/σ_{h0}, ζ=2	20	0	7.3896	7.5430	7.6765	7.7939	7.8978	7.9905	8.0737	8.1487	8.2167	8.2786	8.3353
		10	8.7184	8.8943	9.0470	9.1807	9.2987	9.4037	9.4976	9.5821	9.6585	9.7280	9.7914
		20	10.2643	10.4643	10.6372	10.7880	10.9206	11.0382	11.1431	11.2373	11.3223	11.3994	11.4697
	30	0	8.3553	8.4879	8.6020	8.7010	8.7879	8.8647	8.9330	8.9942	9.0494	9.0993	9.1448
		10	9.9168	10.0656	10.1931	10.3033	10.3997	10.4846	10.5600	10.6273	10.6879	10.7426	10.7923
		20	11.7227	11.8870	12.0269	12.1476	12.2527	12.3449	12.4266	12.4994	12.5647	12.6235	12.6769
		30	13.7245	13.9018	14.0522	14.1813	14.2933	14.3913	14.4778	14.5547	14.6234	14.6853	14.7413
	40	0	9.1140	9.2164	9.3036	9.3786	9.4438	9.5011	9.5517	9.5969	9.6373	9.6738	9.7069
		10	10.8391	10.9511	11.0461	11.1276	11.1982	11.2601	11.3146	11.3632	11.4066	11.4457	11.4811
		20	12.8133	12.9332	13.0343	13.1208	13.1956	13.2608	13.3183	13.3692	13.4147	13.4556	13.4926
		30	14.9703	15.0951	15.2000	15.2893	15.3662	15.4331	15.4919	15.5440	15.5903	15.6319	15.6694
		40	17.2000	17.3262	17.4317	17.5213	17.5982	17.6649	17.7234	17.7750	17.8209	17.8619	17.8989
	50	0	9.6581	9.7284	9.7877	9.8385	9.8823	9.9206	9.9544	9.9843	10.0111	10.0351	10.0569
		10	11.4963	11.5716	11.6349	11.6889	11.7355	11.7761	11.8118	11.8434	11.8716	11.8970	11.9198
		20	13.5791	13.6575	13.7232	13.7791	13.8272	13.8691	13.9058	13.9383	13.9672	13.9932	14.0165
		30	15.8262	15.9053	15.9714	16.0275	16.0756	16.1174	16.1540	16.1863	16.2150	16.2407	16.2639
		40	18.1167	18.1940	18.2585	18.3129	18.3595	18.3999	18.4352	18.4663	18.4940	18.5187	18.5409
		50	20.3005	20.3741	20.4353	20.4868	20.5308	20.5688	20.6019	20.6311	20.6570	20.6801	20.7008